Regions of β2 and β4 Responsible for Differences between the Steady State Dose-Response Relationships of the α3β2 and α3β4 Neuronal Nicotinic Receptors

B. N. COHEN,* A. FIGL,‡ M. W. QUICK,§ C. LABARCA,§ N. DAVIDSON,§ and H. A. LESTER§

From the *Division of Biomedical Sciences, University of California, Riverside, Riverside, California 92521-0121; ‡Division of Chemistry and Chemical Engineering and §Division of Biology, California Institute of Technology, Pasadena, California 91125

ABSTRACT We constructed chimeras of the rat β2 and β4 neuronal nicotinic subunits to locate the regions that contribute to differences between the acetylcholine (ACh) dose-response relationships of the α3β2 and α3β4 receptors. Expressed in *Xenopus* oocytes, the α3β2 receptor displays an EC_{50} for ACh ~20-fold less than the EC_{50} of the α3β4 receptor. The apparent Hill slope (n_{app}) of α3β2 is near one whereas the α3β4 receptor displays an n_{app} near two. Substitutions within the first 120 residues convert the EC_{50} for ACh from one wild-type value to the other. Exchanging just β2:104–120 for the corresponding region of β4 shifts the EC_{50} of ACh dose-response relationship in the expected direction but does not completely convert the EC_{50} of the dose-response relationship from one wild-type value to the other. However, substitutions in the β2:104–120 region do account for the relative sensitivity of the α3β2 receptor to cytisine, tetramethylammonium, and ACh. The expression of β4-like (strong) cooperativity requires an extensive region of β4 (β4:1–301). Relatively short β2 substitutions (β2:104–120) can reduce cooperativity to β2-like values. The results suggest that amino acids within the first 120 residues of β2 and the corresponding region of β4 contribute to an agonist binding site that bridges the α and β subunits in neuronal nicotinic receptors.

INTRODUCTION

Both the α and non-α subunits of the nicotinic acetylcholine receptor (nAChR) play a role in the activation of the receptor by agonist (reviewed in Deneris, Connolly, Rogers, and Duvoisin, 1991; Karlin, 1993; Papke, 1993). Although many studies show that agonist binds to the α subunit (reviewed in Karlin, 1993), present opinion is divided about the possibility of an agonist binding site at the α/non-α subunit interface (Cockcroft, Osguthorpe, Barnard, and Lunt, 1990; Karlin, 1993; Unwin, 1993). The evidence for an α-only binding site is that 9-Å images of *Torpedo* nAChRs

Address correspondence to Henry A. Lester, Division of Biology, California Institute of Technology, Pasadena, CA 91125.

J. GEN. PHYSIOL. © The Rockefeller University Press · 0022-1295/95/06/0745/20 $2.00
Volume 105 June 1995 745–764

reveal a unique cleft within the α subunit that could act as an agonist binding pocket (Unwin, 1993). However, there is no evidence that agonists actually bind within this cleft and contact only α-subunit residues. On the other hand, previous experiments show that (*a*) the muscle-type α subunit (α1) binds nicotinic agonists with appreciable affinities only if it is complexed with a non-α subunit (Blount and Merlie, 1988) and (*b*) the competitive antagonist *d*-tubocurarine (*d*TC) photolabels residues on the γ and δ subunits of *Torpedo* nAChRs (Pedersen and Cohen, 1990; Chiara and Cohen, 1992), which is strong evidence for a direct participation of the non-α subunits in an agonist binding site. However, *d*TC is a larger molecule than ACh and may not contact exactly the same residues that ACh does. Large quantities of purified neuronal nAChRs are not available for direct biochemical and structural analyses of potential agonist binding sites. We have exploited the fact that α3β2 and α3β4 neuronal nAChRs expressed in *Xenopus* oocytes display different relative sensitivities to the ganglionic agonists, cytisine (CYT), tetramethylammonium (TMA), acetylcholine (ACh) and nicotine (Leutje and Patrick, 1991; Figl, Cohen, Quick, Davidson, and Lester, 1992), and different dose-response relationships for ACh (Couturier, Erkman, Valera, Rungger, Bertrand, Boulter, Ballivet, and Bertand, 1990; Cachelin and Jaggi, 1991; Leutje, Piattoni, and Patrick, 1993; Wong, Mennerick, Clifford, Zorumski, and Isenberg, 1993), to locate the residues of β2 and β4 involved in agonist activation of the receptor.

In an earlier study on coexpressed α3 and β subunits, we used β4·β2 chimeras. Extending the β4 NH_2-terminal region of a chimera from residues β4:1–105 to β4:1–122 (Fig. 1) changed the CYT/ACh and TMA/ACh response ratios from α3β2-like (β2-like) to α3β4-like (β4-like) levels (Figl et al., 1992). These data suggested that β4:106–122, and the corresponding region of β2 (β2:104–120), contributes to an agonist binding site that bridges the α and non-α subunits. To test this hypothesis, we have extended the earlier studies with (*a*) more chimeric and mutated β subunits and (*b*) electrophysiological measurements of the agonist dose-response relationship, which we summarize by the half-maximal agonist concentration (EC_{50}) and Hill coefficient (n_{app}). The results show that the region of β4 that converts the EC_{50} for ACh from a β2-like to a β4-like value overlaps the previously localized region that converts the CYT/ACh response ratios of β4 NH_2-terminal chimeras from β2-like to β4-like values (Figl et al., 1992) and suggest that an important component of the agonist binding site lies within the first 120 residues of β2 and the corresponding region of β4. Some of our results have been reported previously in abstract form (Figl, Cohen, Gollub, Davidson, and Lester, 1993).

METHODS

Construction of the β Chimeras and Mutants

We created chimeras between the β2 and β4 subunits by taking advantage of shared restriction sites in the two subunits and using the polymerase chain reaction (PCR) to generate overlapping cDNA fragments (Higuchi, 1990) from the two subunits. Fig. 1 shows an alignment of β2 and β4 amino-acid sequences. Most of the chimeras contained the NH_2-terminal region from one β subtype joined to the succeeding COOH-terminal residues from the other β subtype (NH_2-terminal chimeras). We refer to the NH_2-terminal chimeras in the text by

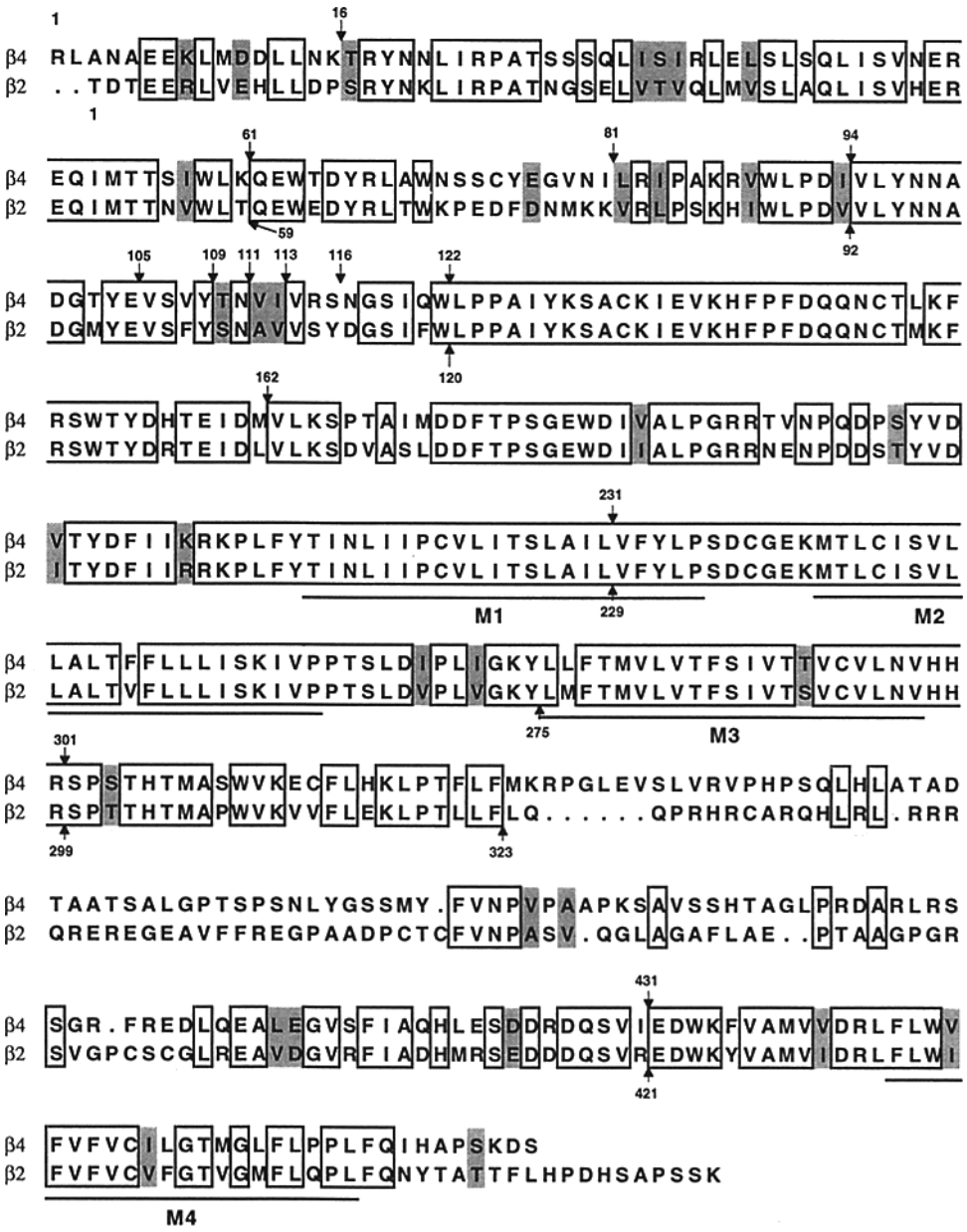

FIGURE 1. The aligned amino acid sequences of the rat β2 and β4 neuronal nAChR subunits. The boxes outline identical residues and the shading denotes homologous residues. Residue 1 begins after the termination of the leader sequences (not shown). The arrows above the β4 sequence point to the transitions in the β4 NH_2-terminal chimeras between the β4 and β2 sequence. The arrows beneath the β2 sequence point to the transitions in the β2 NH_2-terminal chimeras between the β2 and β4 sequence. The numbers above (below) the arrows are the last residues in the β4 (β2) NH_2-terminal regions of the chimeras. The lines beneath the β2 sequence denote the transmembrane regions M1–M4.

transition points between the two types of β subunits. For example, β2(229)·β4 is a chimera containing the first 229 residues of β2 joined to residues 232–475 of β4 (see Fig. 1). Chimeras containing internal substitutions are labeled by the end points of the substitution. For example, β4·β2(104–120)·β4 is a chimera in which we substituted β2:104–120 for residues 106–122 of the β4 subunit (these labels have been shortened to β2(104–120) and β4(106–122) in Figs. 7 and 8).

To create the β2(229)·β4 and β4(231)·β2 chimeras, we excised the cDNA fragments for residues β2:1–229 and β4:1–231 from the wild-type subunits with EcoRI and BbsI, subcloned the excised fragments into the complementary restricted plasmid from the opposite β subunit, and sequenced the region around the β4/β2 transition to check the final product. The remaining chimeras were constructed in three steps: (*a*) we synthesized two or more separate PCR fragments; (*b*) we annealed and amplified the PCR fragments; and (*c*) we inserted the annealed fragment into the appropriate restriction sites in the wild-type plasmid. We normally introduced a silent mutation into the chimera during the initial PCR reaction to allow us to check the final product by restriction analysis. In addition, all the chimeras were verified by DNA sequencing. We made point mutations using the Altered Sites Kit (Promega Corp., Madison, WI) and verified the mutations by restriction analysis and DNA sequencing. Point mutations are denoted in the text by subscripts that contain the single letter code for the original residue, followed by its position in the sequence, and the residue to which it was mutated. We synthesized mRNA in vitro using the MEGAscript Kit (Ambion, Austin, TX) or a previously published method (Guastella, Nelson, Nelson, Czyzyk, Keynan, Midel, Davidson, Lester, and Kanner, 1990) and checked the size of the synthesized mRNA by agarose gel electrophoresis.

Oocyte Expression

Stage V–VI *Xenopus* oocytes were isolated as described previously (Quick and Lester, 1994) and injected with mRNA in a stoichiometric ratio for α:β of 2:3. The amount of mRNA injected ($\leq$25 ng/subunit) was adjusted to maintain a maximum response (I_{max}) of $\leq$10 μA at −50 mV. Before recording, the oocytes were incubated for 2–7 d at 18°C in a modified Barth's solution supplemented with 50 μg/ml gentamicin, 2.5 mM pyruvate, and 5% horse serum (Quick and Lester, 1994).

Electrophysiological Recordings

The oocytes were voltage clamped at −50 mV with two, 3 M KCl-filled microelectrodes made from thick-walled borosilicate glass (model BF150-86-10, Sutter Instrument Co., Novato, CA) and an AxoClamp 2A voltage clamp (Axon Instruments, Foster City, CA). During the experiments, we perfused the recording chamber ($\sim$1.5 ml vol) with 98 mM NaCl, 1 mM $MgCl_2$, and 5 mM HEPES (pH 7.4) at room temperature (20–24°C) at 10–20 ml/min. We omitted Ca^{2+} from the recording solution because the entry of Ca^{2+} through neuronal nAChRs can activate the endogenous Ca^{2+}-activated Cl^- current of the oocyte (Vernino, Amador, Leutje, Patrick, and Dani, 1992).

We applied agonists to the oocytes by pinching-off the outflow of a U tube (Bormann, 1992) with a solenoid-activated pinch valve (Cole-Palmer, Niles, IL) under computer control. The time constant of the approach to a steady state response (τ_{on}) was 0.4–0.5 s at slowly desensitizing agonist doses. To check the effective [agonist] reaching the oocyte from the U tube, we applied a slowly desensitizing dose of ACh (1 μM) to an oocyte expressing α3β2 using the bath and U tube perfusion systems. Bath and U tube application of 1 μM ACh produced the same steady state response. Endogenous muscarinic responses were rare and easily identified by their oscillatory nature and delayed onset after agonist application from the U tube. We did not use oocytes exhibiting muscarinic responses.

Collection and Analysis of the Dose-Response Data

We recorded the responses to 6–11 different agonist doses to measure the dose-response relationships for individual oocytes. The agonist was applied in 6-s pulses separated by a 2–3-min rinse with control saline. The responses were filtered at 20 Hz and digitized at a sampling frequency of 50 Hz using an MS-DOS computer equipped with pCLAMP V5.5 software (Axon Instruments).

We fit the dose-response data for individual oocytes to the Hill equation,

$$I_{peak} = \frac{I_{max}}{1 + \left(\frac{EC_{50}}{[A]}\right)^{n_{app}}},$$

where I_{peak} was the peak response at agonist concentration $[A]$, using weighted nonlinear least-squares regression. To reduce the interdependence of the parameters I_{max}, EC_{50}, and n_{app}, we allowed only the I_{max} and the EC_{50} to vary when fitting to the Hill equation. The n_{app} was fixed at the mean slope of the Hill plots for the receptor subtype being fit. The n_{app} was determined (*a*) from the Hill plot by linear regression of $\log[I_{peak}/(I_{max} - I_{peak})]$ against log[agonist] where I_{max} was the maximum observed response and (*b*) from the log–log plot by regression at the foot of the dose-response relationship. The correlation between these two measurements of the n_{app} was 0.89 for the 26 receptor types discussed in the text. Regression of the log–log slope against the corresponding Hill slope predicted a log–log slope of 1.1 for a Hill slope of 1.0 and a log–log slope of 1.9 for a Hill slope of 2.0. We preferred the estimates of the n_{app} from the Hill plot because (*a*) the slope of the Hill plot was based on more points per oocyte than the initial log–log slope measurements, (*b*) log–log slope measurements tend to underestimate the true n_{app}, (*c*) the Hill plot included more data points with a higher signal/noise ratio than the initial log–log plot, and (*d*) the n_{app}'s from the Hill plot generally fit the dose-response relationship better than the n_{app}'s from the log–log plots. The n_{app}'s reported in the text are from Hill slopes rather than from log–log slopes unless stated otherwise. We weighted the residuals by $1/\sqrt{I_{peak}}$ for the fit to the Hill equation because the variance of I_{peak} at the high end of the dose-response relationship was larger than the variance of I_{peak} at the low end. Repeated measurements on a single oocyte showed that long-term desensitization reduced the I_{max} but did not affect the EC_{50} or n_{app}.

To compare measurements of the EC_{50} with widely different variances, we transformed the EC_{50}'s to log values. Unless otherwise stated, the measurement errors reported in the text are standard deviations (SDs) and the SDs for the EC_{50}'s given in the text are for untransformed data. To construct normalized dose-response relationships for the receptors, we normalized the individual dose-response relationships to the fitted I_{max}'s and pooled the resulting data. We then refit the Hill equation allowing only the EC_{50} to vary. The error reported for the normalized EC_{50} measurements is the standard error of estimate (SEE).

Correction of the Peak Response for Desensitization

Rapid desensitization reduces the peak response because some receptors desensitize while the [agonist] is still rising around the oocyte. We used the following three-state scheme (Scheme I) to calculate depression of the peak response by rapid desensitization,

$$C \xrightarrow{k_1} O \xrightarrow{k_2} D,$$

SCHEME I

where C, O, and D are the closed, open, and desensitized states of the receptor, k_1 is the rate constant for the [ACh] to reach a steady state around the oocyte, and k_2 represents the rate constant for desensitization. We obtained k_1 directly from the rate constant of the rising phase of the response with 1 μM ACh and k_2 directly from the rate constant of the decay of the response within the agonist pulse (in the Results section, $1/k_1$ and $1/k_2$ are termed τ_{on} and τ_{desen}). The relationship between the peak amplitude of the observed response (I_{peak}) and the peak amplitude of the calculated response (I_{calc}) is,

$$I_{calc} = \frac{I_{peak}}{\frac{k_1}{k_2 - k_1}\left[\left(\frac{k_1}{k_2}\right)^{k_1/(k_2-k_1)} - \left(\frac{k_1}{k_2}\right)^{k_2/(k_2-k_1)}\right]} \quad (1)$$

At high [ACh]'s, the decay of the response consisted of two exponential components. These components were corrected separately using Eq. 1 and then summed to obtain the final calculated peak response.

RESULTS

The β Subunit Affects the Agonist Dose-Response Relationship

Consistent with previous data (Couturier et al., 1990; Leutje et al., 1993; Wong et al., 1993), we found that the β subunit profoundly affects the sensitivity of neuronal nAChRs to ACh. Expressing α3 with β2, instead of with β4, shifted the ACh dose-response relationship at −50 mV considerably to the left and reduced its slope (Fig. 2). The traces in Fig. 2, *A* and *B*, are typical ACh responses of α3β2 (Fig. 2 *A*) and α3β4 (Fig. 2 *B*) from oocytes with similar maximum responses. We fit the ACh

FIGURE 2. (*opposite*) Expressing α3 with β2, rather than with β4, reduces the EC_{50} and apparent Hill coefficient (n_{app}) of the ACh dose-response relationship. (*A*) Responses of α3β2 to 1–300 μM ACh. The numbers are the [ACh] in μM. The square pulse above the traces is the duration of the application of ACh from the U tube. (*B*) Responses of α3β4 to 20–1,000 μM ACh. (*C*) Dose-response plots for α3β2 and α3β4. The symbols denote different oocytes expressing α3β2 (*filled circles, open circles, filled inverted triangles, open inverted triangles, filled squares*) or α3β4 (*open squares, filled upright triangles, open upright triangles*). The lines are fits to the Hill equation (see Methods). The EC_{50}'s and the I_{max}'s are 17 μM and 1,863 nA (*filled circles*), 13 μM and 1,757 nA (*open circles*), 15 μM and 2,056 nA (*filled inverted triangles*), 9 μM and 1,461 nA (*hollow inverted triangles*), 13 μM and 1,498 nA (*filled squares*), 216 μM and 1,944 nA (*open squares*), 232 μM and 2,061 nA (*filled upright triangle*), and 209 μM and 2,100 nA (*open upright triangle*). Voltage = −50 mV. (*D*) Hill plots for the peak ACh responses (I_{peak}) of α3β2 and α3β4. I_{max} is the maximum observed I_{peak}. The symbols denote different oocytes; α3β2 (*filled circles, hollow circles*), α3β4 (*filled inverted triangles, hollow inverted triangles, filled squares*). Overlap obscures some of the data. The n_{app}'s are 0.9 (*filled circles*), 1.0 (*open circles*), 2.2 (*filled inverted triangles*), 2.3 (*inverted triangles*), and 2.2 (*filled squares*). (*E*) Log–log plots of the foot of the ACh dose-response relationship show that the slope of the α3β4 log dose-log response relationship is ~twice that of α3β2. The symbols represent data from six oocytes (each oocyte is represented by a different symbol). The lines are regression lines fit to the log–log data. The slopes for α3β4 are 2.0 (*filled circles*), 2.0 (*open circles*), and 1.8 (*filled inverted triangles*); the slopes for α3β2 are 1.1 (*hollow inverted triangles*), 1.0 (*filled squares*), and 1.0 (*hollow squares*).

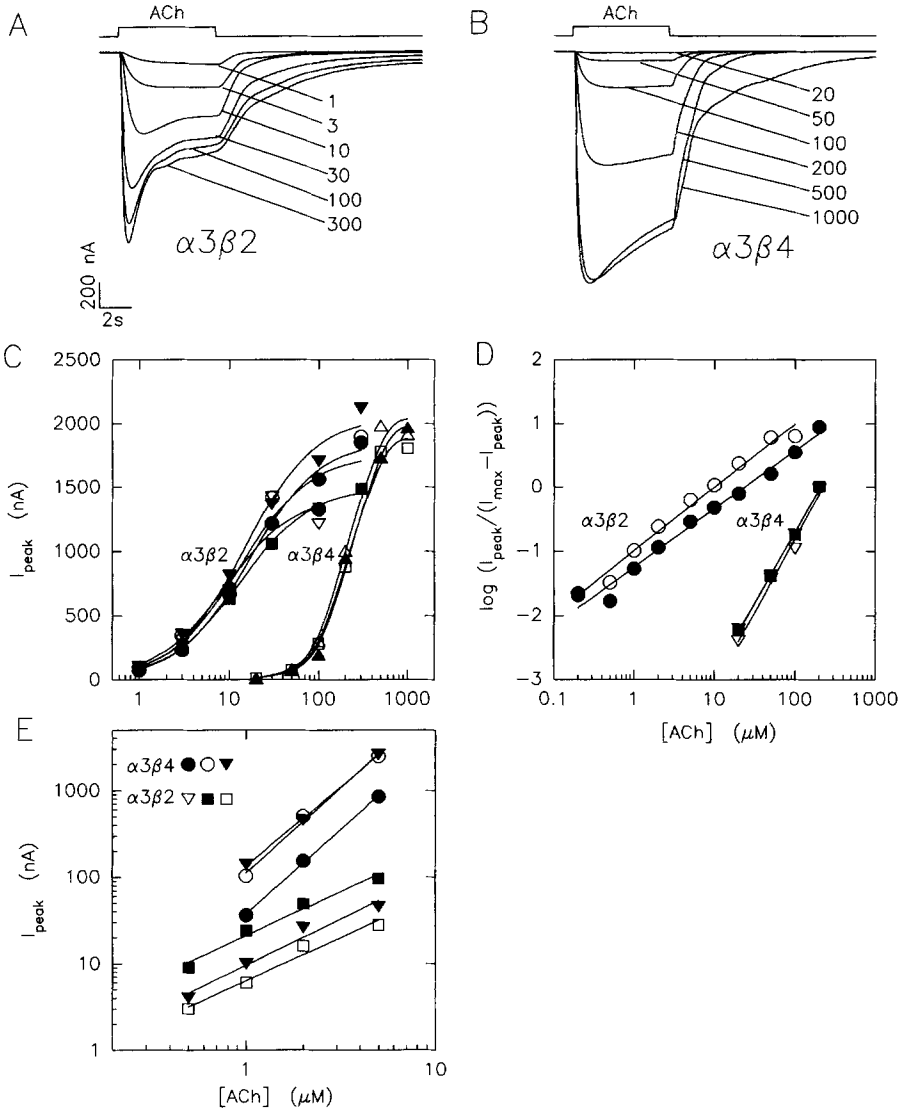

FIGURE 2

dose-response relationships for α3β2 and α3β4 to the Hill equation (Fig. 2 *C*) using the n_{app}'s for α3β2 and α3β4 determined from Hill plots of the ACh responses (Fig. 2 *D*). Similar to previous results (Couturier et al., 1990; Leutje et al., 1993; Wong et al., 1993), the EC_{50} for ACh was 11 ± 4 μM (mean ± SD, n = 29 oocytes) for the rat α3β2 receptor and 219 ± 12 μM (n = 3) for the rat α3β4 receptor. The n_{app} for α3β2 was 1.1 ± 0.2 (n = 29) and the n_{app} for α3β4 was 2.2 ± 0.1 (n = 3). Fig. 2 *D* shows Hill plots for the two receptors. Measurements of the n_{app} from the initial slope of a log–log plot of the dose-response relationship (where desensitization and agonist

self-block are minimal) gave similar, but slightly smaller, n_{app}'s for α3β2 (0.9 ± 0.1, n = 11) and α3β4 (1.9 ± 0.1, n = 3). Fig. 2 *E* shows examples of the initial portions of the log(dose)–log(response) relationships for the two wild-type receptors. The agreement of these measurements shows that the difference between the n_{app}'s of α3β2 and α3β4 was not due to desensitization or open-channel block by the agonist. Injecting equal amounts of mRNA generally gave much larger maximal ACh responses for α3β4 than for α3β2 (~10-fold) but we did not study these differences further.

The dose-response relationships of α3β2 and α3β4 for TMA displayed differences comparable to, but less pronounced than, those for ACh (Fig. 3). Fig. 3, *A* and *B*, shows sample responses of α3β2 (Fig. 3 *A*) and α3β4 (Fig. 3 *B*) to TMA. Rapid desensitization is less pronounced for both wild-type receptors with TMA as the agonist. The EC_{50} of α3β2 for TMA (76 ± 11 μM, n = 7) was fivefold smaller than that of α3β4 (424 ± 94 μM, n = 6) and the n_{app} of α3β2 for TMA (1.4 ± 0.1, n = 7) determined from Hill plots of the dose-response data was significantly smaller than the n_{app} of α3β4 (2.0 ± 0.2, n = 6). As with ACh, the β2 subunit shifts the TMA dose-response considerably to the left (Fig. 3 *C*). Thus, the β subunit affects the activation of neuronal nAChRs by an agonist that contains only the quaternary ammonium portion of the ACh molecule; and the effects of the β subunit on the agonist dose-response relationship persist even with an agonist that desensitizes the receptor more slowly than ACh.

Rapid Desensitization Fails to Account for Differences in the EC_{50}'s of α3β2 and α3β4

The response of α3β2 to ACh (Fig. 2 *A*) desensitized more quickly than the response of α3β4 to ACh (Fig. 2 *B*). The time constant τ_{on} for activation of the α3β2 response to 1 μM ACh to reach a steady state was 0.4–0.5 s. The time constant τ_{desen} for the desensitization of the α3β2 response decreased from 5–7 s at 3 μM ACh to 0.6–0.8 s at 300 μM ACh. Desensitization of the α3β2 response to 300 μM ACh was biphasic with an additional slow time constant of 5–6 s. The α3β4 receptor displayed little desensitization during the 6-s agonist pulse. The τ_{desen} for α3β4 was 5–6 s at 1–2 mM ACh and was too slow to measure at 20–500 μM ACh.

We corrected the peak ACh response of the wild-type receptors for apparent desensitization (see Methods) and fit the corrected data to the Hill equation to determine how much of the difference in the EC_{50}'s could be due to a difference in the rate of desensitization. Correcting the peak response of α3β2 for apparent desensitization left n_{app} unchanged but increased the EC_{50} of α3β2 for ACh twofold. Desensitization of α3β4 did not significantly affect the ACh dose-response relationship. Thus, allowing for the potential effects of desensitization, the EC_{50} of α3β4 for ACh was still 10-fold larger than the EC_{50} of α3β2. The differences in desensitization accounted for such a small fraction of the differences between the EC_{50}'s of the wild-type receptors that we decided not to attempt to correct the amplitudes of the peak responses. We were unable to resolve desensitization occurring on a time scale faster than 1 s (Maconochie and Knight, 1992) using our drug application system (see

Methods). Such desensitization would produce an apparent decrease in the EC_{50} of the dose-response relationship in our experiments.

NH_2-Terminal Substitutions of 105 or More β4 Residues Increase the EC_{50} for ACh

Substitutions of 94 or fewer β4 residues had only small effects on the EC_{50} for ACh (Fig. 4 *A*); the EC_{50}'s of the α3β4(16)·β2, α3β4(81)·β2, and α3β4(94)·β2 chimeras for

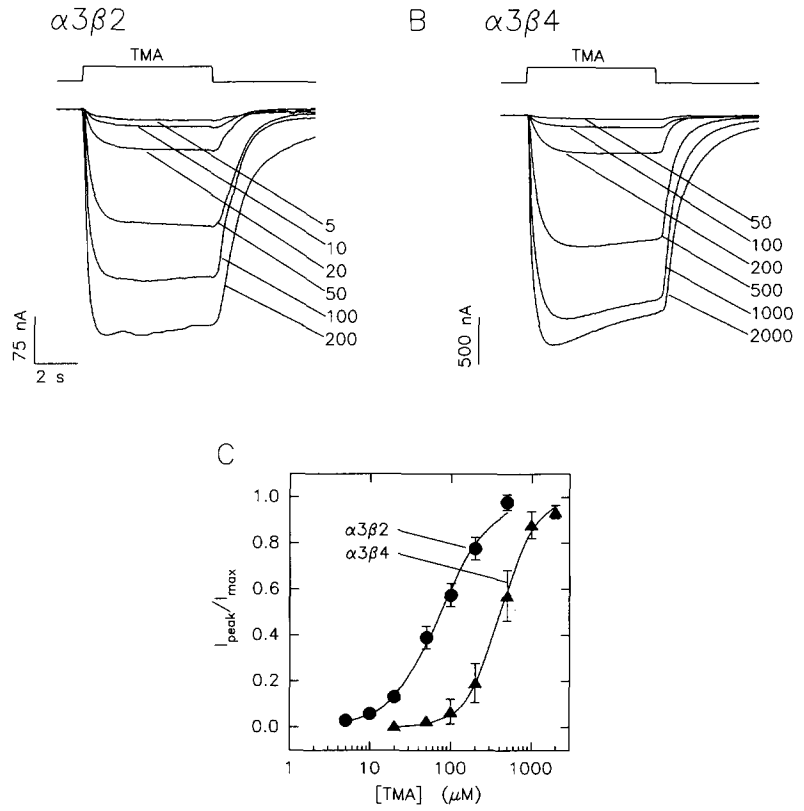

FIGURE 3. Expressing α3 with β4, rather than with β2, increases the EC_{50} and the n_{app} of the TMA dose-response relationship. (*A*) Responses of α3β2 to 5–200 μM TMA. The responses are labeled with the [TMA] in μM. The square pulse above the traces shows the timing of the TMA application. (*B*) Responses of α3β4 to 50–2,000 μM TMA. (*C*) Expression with β4 shifts the TMA dose-response relationship to the right and increases its slope. The symbols are mean normalized responses ± SD. The EC_{50}'s of the TMA dose-response relationships for α3β2 and α3β4 are 75 ± 3 μM (n = 7) and 416 ± 12 μM (n = 6) (± standard error of estimate, ±SEE).

ACh (13–18 μM) were within a factor of two of the EC_{50} of α3β2 for ACh. However, if the β4 NH_2-terminal region of the chimeras was extended from 94 to 109 residues, the EC_{50} for ACh increased dramatically to a β4-like value. Fig. 4 *B* presents data for the interesting region between residues β4:94 and β4:109 and shows the rightward shift of the normalized ACh dose-response relationships as more β4 residues are

included. All the β4 NH_2-terminal chimeras with 113 or more β4 NH_2-terminal residues displayed β4-like EC_{50}'s for ACh (> 10-fold larger than that of α3β2). Thus, the β4/β2 residue substitutions necessary for β4-like ACh sensitivity in the β4·β2 chimeras lie in the first 113 residues of β4.

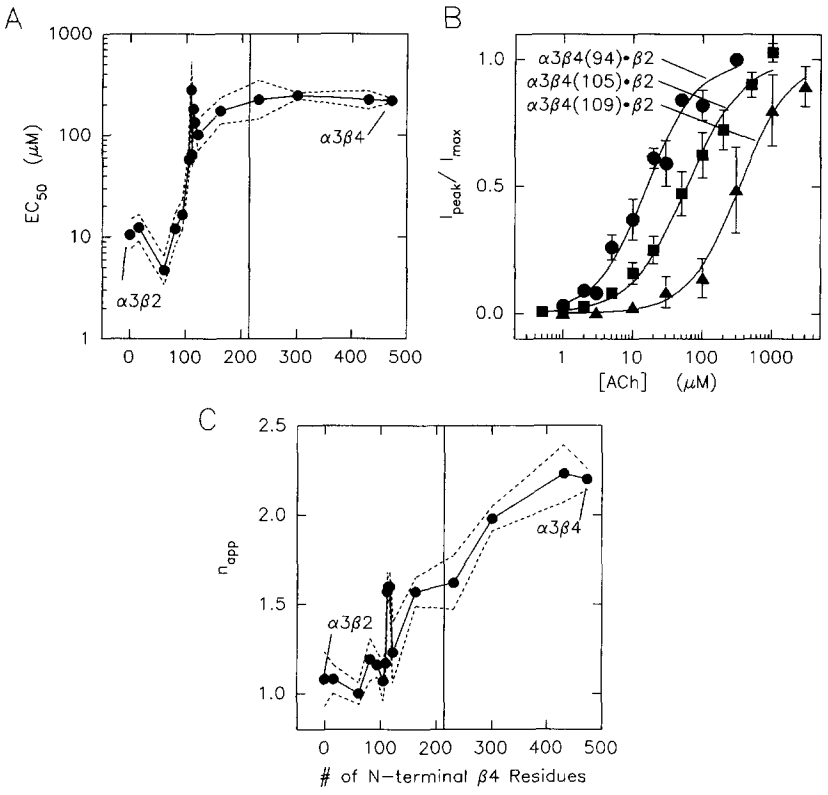

FIGURE 4. (*A*) Substituting 105 or more β4 NH_2-terminal residues for the corresponding region of β2 increases the EC_{50} for ACh. The horizontal axis is the number of β4 NH_2-terminal residues in the chimera: zero for α3β2 and 475 for α3β4. The symbols are the mean values for the two wild types and 14 β4·β2 chimeras (n = 2–29 oocytes). Overlap obscures some of the data. The dashed lines are 1 ± SD. The means and SDs for the EC_{50}'s were computed from log transformed data. The vertical line denotes the beginning of M1. (*B*) The addition of two residue substitutions in the β4:95–109 sequence (see Fig. 1) shifts the ACh dose-response relationship dramatically to the right. The symbols are the mean normalized responses ± SD (see Methods) for α3β4(94)·β2, α3β4(105)·β2, and α3β4(109)·β2. The lines are fits to the Hill equation (see Methods). The EC_{50}'s for ACh are 16 ± 1 μM (n = 9), 60 ± 4 μM (n = 4), and 338 ± 23 μM (n = 6), respectively (±SEE). (*C*) Substituting ≥301 β4 NH_2-terminal residues increases the n_{app} for ACh to ≥2.0.

There are only two β4/β2 residue substitutions in β4:95–109 (see Fig. 1). The addition of these two substitutions increased the EC_{50} of the β4 NH_2-terminal chimeras from β2-like to β4-like levels. Therefore, we made the site-directed mutations $\beta2_{M101T,F106V}$ to change just these residues in the β2 subunit. The EC_{50} of

the mutated receptor for ACh (19 ± 4 μM, $n = 5$) was within a factor of two of the value for α3β2 (11 ± 4 μM). Thus, the increase in the EC_{50} of α3β4(109)·β2 over the EC_{50} of α3β4(94)·β2 depended on residue substitutions within the first 94 residues of β4 in addition to the two substitutions β2:Met101↔β4:Thr103 and β2:Phe106↔β4:Val108. Previous experiments (Chiara et al., 1992; O'Leary, Filatov, and White, 1994) also suggest that a tryptophan (γ:Trp55, δ:Trp57) in the first 60 residues of the non-α subunits contributes to the agonist binding sites of the *Torpedo* nAChR.

We also made the mutation $\alpha3\beta4(61)_{S28N}\cdot\beta2$ to determine if the loss of a potential glycosylation site at β2:Asn26 was responsible for the slight decrease in the EC_{50} of α3β4(61)·β2 below that of α3β2. The EC_{50} (6 ± 3 μM, $n = 4$) and n_{app} (0.8 ± 0.1, $n = 4$) of $\alpha3\beta4(61)_{S28N}\cdot\beta2$ for ACh were not significantly different from the EC_{50} (5 ± 1 μM, $n = 6$) and the n_{app} (1.0 ± 0.1, $n = 6$) of α3β4(61)·β2. Thus, the removal of a potential glycosylation site at β2:Asn26 was not responsible for the effect of α3β4(61)·β2 on the EC_{50} for ACh.

Increasing the n_{app} to β4-like Values Requires an Extensive Region of β4

The n_{app} of the β4·β2 chimeras showed a more gradual dependence on the β4/β2 transition point than the EC_{50}. The n_{app}'s of these chimeras fell into three categories, β2-like (n_{app} = 1.0–1.2), intermediate (n_{app} = 1.6), and β4-like (n_{app} = 2.0–2.2). The chimeras containing 109 or less β4 NH_2-terminal residues exhibited β2-like n_{app}'s; the chimeras containing 109–231 β4 NH_2-terminal residues exhibited intermediate n_{app}'s except for α3β4(122)·β2 (n_{app} = 1.2 ± 0.2, $n = 2$); and the chimeras containing 301 or more β4 NH_2-terminal residues exhibited β4-like n_{app}'s. The $\beta2_{M101T,F106V}$ mutation did not affect the n_{app} for ACh.

We are not surprised by the differences between the regions of β4 that affect the EC_{50} and those that affect the n_{app}. Areas of contact between the subunits outside the agonist binding site may affect the cooperativity of a multisubunit receptor (Koshland, Neméthy, and Filmer, 1966). Nevertheless, the overlap between the β4 residues that increase the EC_{50}'s of the β4·β2 chimeras and the residues that increase the n_{app} from β2-like to intermediate values suggests that β4:106–122 and β2:104–120 may be areas where the α and β subunits contact each other. The results for the β4 NH_2-terminal chimeras also suggest that these subunits contact each other somewhere between the end of the first putative transmembrane domain M1 and the initial portion of the M3–M4 intracellular loop. However, our data do not allow us to exclude the alternative hypothesis that these residue substitutions produce a conformational change in the receptor that affects cooperativity indirectly.

Substituting β2:1–120 for the Corresponding Region of β4 Reduces the EC_{50} to a β2-like Value

We constructed a number of β2·β4 chimeras to determine the region of the β2 subunit required to reduce the EC_{50} of the chimeras to β2-like values (Fig. 5 *A*). Similar to results for the β4·β2 chimeras, substituting the first 120 residues of β2 for the corresponding region of β4 reduced the EC_{50} for ACh to 16 ± 8 μM ($n = 3$) which resembles the EC_{50} of α3β2 (11 ± 4 μM). Fig. 5 *B* shows the effect of this substitution on the ACh dose-response relationship. Substituting the first 92 residues of β2 also reduced the EC_{50} for ACh (Fig. 5 *A*). Thus, residue substitutions in the first

92 amino acids of β2 do affect the sensitivity of the receptor to agonist but this effect is masked in the β4 NH_2-terminal chimeras.

There is an anomalous member of the β2·β4 series; the EC_{50} of α3β2(229)·β4 for ACh was close to that of α3β4 (Fig. 5 *A*). This anomalous EC_{50} does not seem to be

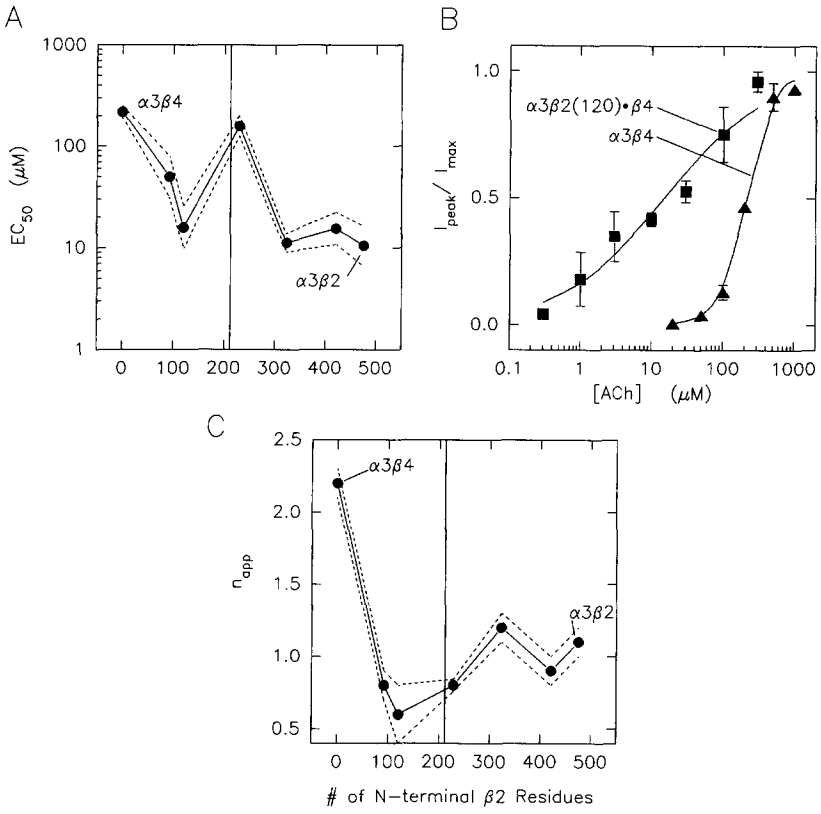

FIGURE 5. (*A*) β2 NH_2-terminal substitutions have a more complex effect on the EC_{50} for ACh than β4 NH_2-terminal substitutions. The symbols are mean values for the two wild types and five β2 NH_2-terminal chimeras (n = 3–29). The dashed lines are ± SD. The vertical line denotes the beginning of M1. (*B*) Substituting β2:1–120 for the corresponding region of β4 reduces the EC_{50} to a β2-like value. The symbols are the normalized responses ± SD. The lines are fits to the Hill equation. The EC_{50}'s for α3β2(120)·β4 and α3β4 are 15 ± 3 μM (n = 3) and 215 ± 8 μM (n = 3) (± SEE). (*C*) Substituting 93 or more β2 NH_2-terminal residues for the corresponding regions of β4 reduces the n_{app} for ACh to β2-like values.

due to a disruption of the agonist binding site. Previous data show that this chimera displays a β2-like affinity for the irreversible competitive inhibitor, neuronal bungarotoxin (Papke, Duvoisin, and Heinemann, 1993), and we found that α3β2(229)·β4 exhibits a clear β2-like insensitivity to CYT relative to ACh (Fig. 6).

Thus, the results for the β4 and β2 NH_2-terminal chimeras show that β2/β4 substitutions in the first 120 residues of β2 and the first 113 residues of β4 are sufficient to convert the EC_{50} for ACh from one wild-type value to another.

Short β2 NH_2-Terminal Substitutions Disrupt the Cooperativity of the Receptor

β2 NH_2-terminal sequences of 92 or more residues reduced the n_{app} for ACh to a value near that of α3β2 for ACh (1.1 ± 0.2) (Fig. 5 *C*). Moreover, a single measurement of the n_{app} (1.1) for α3β2(59)·β4 from the initial portion of the log–log dose response relationship suggests that even substituting the first 59 residues of β2 for the corresponding region of β4 may suffice to reduce the n_{app} of the chimera to a β2-like value. Thus, as for the β4 NH_2-terminal chimeras, changes in the EC_{50}'s of the β2 NH_2-terminal chimeras were not synchronous with changes in the n_{app}. If the n_{app} is determined by areas of contact between the subunits, then these results suggest that an extensive region of subunit/subunit contacts, particularly at the NH_2-terminals of the α3 and β4 subunits, are required for the receptor to display the strong cooperativity observed for the α3β4 receptor. The small n_{app} of the α3β2(120)·β4 raises the possibility that there may also be heterogeneity in the assembly of this receptor. The α3β2(92)·β4 and α3β2(229)·β4 chimeras also display Hill coefficients that are slightly < 1.

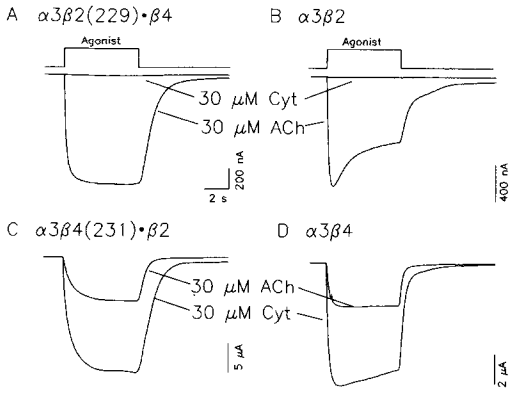

FIGURE 6. The α3β2(229)·β4 chimera displays a β2-like insensitivity to 30 μM CYT relative to ACh. (*A–D*) Responses to 30 μM CYT and 30 μM ACh at −50 mV. The square pulses above the traces denotes the release of agonist from the U tube.

Exchanging Just β2:104–120 and β4:106–122 Shifts the EC_{50} in the Expected Direction

Mutations show that the two β4/β2 substitutions β2:Met101↔β4:Thr103 and β2:Phe106↔β4:Val108 are not sufficient to change the EC_{50} of the ACh dose-response relationship. We therefore constructed the reciprocal chimeras α3β4·β2(104–120)·β4 and α3β2·β4(106–122)·β2 to test whether more extensive substitutions in this area could affect the EC_{50} for ACh. Exchanging β2:104–120 and β4:106–122 shifted the EC_{50} for ACh towards the opposing wild-type value (Fig. 7, *A* and *B*). Substituting β2:104–120 for the corresponding region of β4 reduced the EC_{50} for ACh to 90 ± 20 μM ($n = 4$), a value less than half that of α3β4 (219 ± 12 μM). The reciprocal substitution (β4:106–122 for the corresponding region of β2) increased the EC_{50} about threefold over the EC_{50} for α3β2, to 28 ± 6 μM ($n = 8$). Consistent with the results for the β2 and β4 NH_2-terminal chimeras, substituting β2:104–120 reduced the cooperativity of the chimera to 1.3 ± 0.1 ($n = 4$) while the reciprocal substitution did not significantly increase the n_{app} for ACh (1.3 ± 0.2, $n = 8$). Thus, eight residue

substitutions in β2:104–120 and β4:106–122 (see Fig. 1) had an effect on the EC_{50} and n_{app} for ACh that was independent of substitutions elsewhere in the β subunits.

Substituting β2:104–120 for β4:106–122 Also Affects Agonist Selectivity

Previous data (Figl et al., 1992) show that extending the β4 region of a β4 NH_2-terminal chimera from β4:1–105 to β4:1–122 increases the 30 μM CYT/30 μM ACh (CYT/ACh) and 100 μM TMA/30 μM ACh (TMA/ACh) response ratios from β2-like to β4-like levels. We tested the effects of exchanging β2:104–120 and β4:106–122 to determine whether these regions accounted for the effects of the β4 NH_2-terminal chimeras on agonist selectivity.

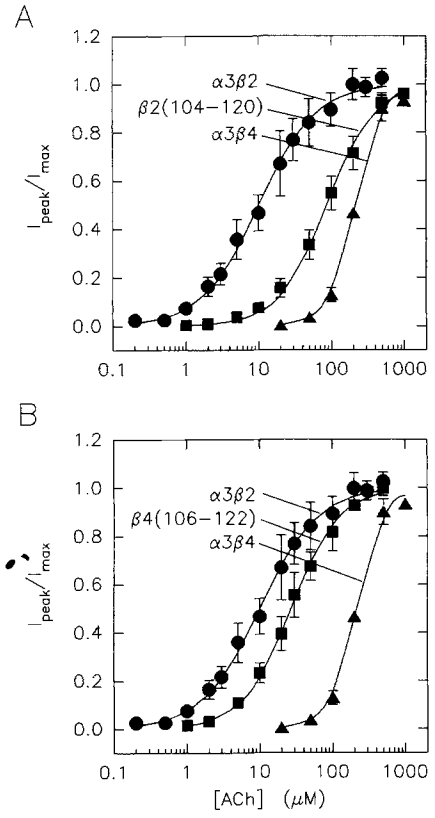

FIGURE 7. Exchanging β2:104–120 and β4:106–122 shifts the EC_{50} of the ACh dose-response relationship in the appropriate direction. (*A*) Substituting β2:104–120 for β4: 106–122 shifts the ACh dose-response relationship to the right of the α3β4 dose-response relationship. (*B*) Substituting β4: 106–122 for β2:104–120 shifts the dose-response relationship to the left of the α3β2 dose-response relationship.

Substituting β2:104–120 for β4:106–122 reduced the CYT/ACh and TMA/ACh response ratios to β2-like values (Fig. 8, *A* and *B*), but the reciprocal substitution β4:106–122 for β2:104–120 produced only a small increase in the CYT/ACh or TMA/ACh response ratios toward β4-like values. Thus, similar to the effects of β2 substitutions on cooperativity, short internal substitutions reduce, but do not restore, the relative sensitivity of the α3β4 receptor to ganglionic agonists such as CYT and TMA. The structural basis for this correspondence between the effects of internal substitutions on agonist selectivity and cooperativity is unclear. Nonetheless, the

effects of exchanging β4:106–122 and β2:104–120 on several measurements associated with agonist activation of the receptor suggest that these areas are places where the α and β subunits contact to form an agonist binding site.

The Sole M2 Substitution Does Not Affect the ACh Dose-Response Relationship

Dose-response relationships for nAChRs are affected by mutations at several residues in the M2 transmembrane domain (reviewed in Karlin, 1993). There is a single β2/β4 substitution in the M2 region (β2:Val253↔β4:Phe255). We made the reciprocal

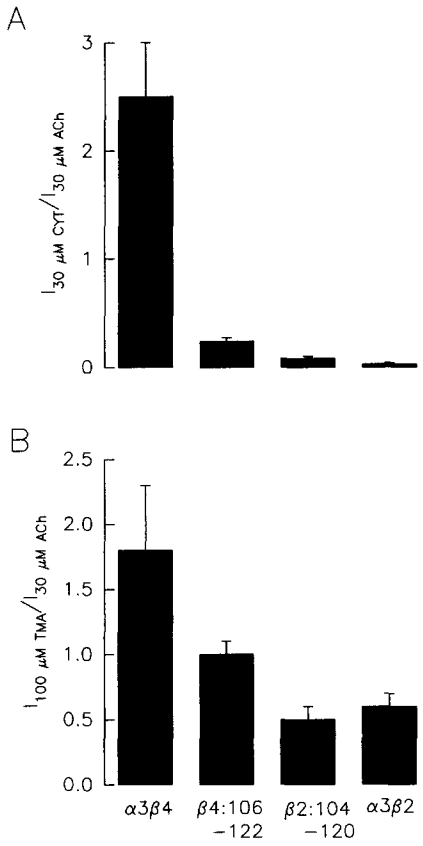

FIGURE 8. Exchanging β2:104–120 and β4:106–122 changes the ratio of the 30 μM cytisine (CYT) and 30 μM ACh responses and the ratio of the 100 μM tetramethylammonium (TMA) and 30 μM ACh responses. (*A*) Substituting β2:104–120 for β4:106–122 reduces the CYT/ACh response ratio to a β2-like value but substituting β4:106–122 for β2:104–120 only marginally increases the CYT/ACh response ratio. The solid bars are means ± SD. (*B*) Substituting β2:104–120 for β4:106–122 reduces the TMA/ACh response ratio to a β2-like value. Substituting β4:106–122 for β2:104–120 increases the TMA/ACh response ratio to an intermediate value.

point mutations $\beta4_{F255V}$ and $\beta2_{V253F}$ to test whether this substitution could shift the agonist dose-response relationship. Neither mutation significantly affected the EC_{50} or n_{app}. The n_{app} of $\alpha3\beta4_{F255V}$ was 2.0 ± 0.1 (n = 3); the n_{app} of $\alpha3\beta2_{V253F}$ was 1.2 ± 0.1 (n = 3); the EC_{50} of $\alpha3\beta4_{F255V}$ was 231 ± 18 μM (n = 3); and, the EC_{50} of $\alpha3\beta2_{V253F}$ was 9 ± 1 μM (n = 3).

DISCUSSION

The data reported in this paper describe the steady state dose-response relations of chimeric and mutated β2 and β4 subunits expressed with the α3 subunit in oocytes.

The data show that the first 120 residues of β2 and a comparable, but slightly shorter, region of β4 largely account for the different EC_{50}'s of the wild-type dose-response relationships. In the sharpest region of transition, chimeras that differ at only two residues have more than a 10-fold difference in the EC_{50}. However, when we examined the corresponding mutant $\beta2_{M101T,F106V}$ it retained the EC_{50} of the wild-type β2 subunit. This important result shows that the two critical residues are interacting with other upstream residues during activation of the receptor. Longer substitutions in this region (β2:104–120↔β4:106–122) do affect (*a*) the ACh dose-response relationship and (*b*) the relative responses to several ganglionic agonists. The domains we have identified that affect the EC_{50} probably affect agonist binding and may contribute to an agonist binding site that bridges the α and β subunits.

Our experiments also bear on the regions responsible for the cooperativity of the receptor (n_{app}). Regions of the β subunits responsible for differences in the n_{app} overlap with, but are not identical to, those responsible for differences in the EC_{50}. The β2:104–120 and β4:106–122 regions affect both measures. However, for the β4 NH_2-terminal chimeras, the transition from β2-like to β4-like cooperativity occurs more gradually than the transition from a β2-like to a β4-like EC_{50} and requires an extensive NH_2-terminal region of the β4 subunit. The high level of cooperativity of α3β4 is disrupted by short β2 substitutions. If receptor cooperativity is determined by areas of contact between the subunits (Koshland et al., 1966), then one of these contact regions appears to lie in β2:104–120 and β4:106–122.

The differences we observed between the ACh dose-response relationships of the α3β2 and α3β4 receptors are similar to those reported previously by Couturier et al. (1990), Leutje et al. (1993), and Wong et al. (1993) but differ substantially from those reported by Cachelin et al. (1991). Cachelin et al. (1991) report a much smaller value for the EC_{50} of α3β4 for ACh (30 μM) and a much larger value for the EC_{50} of α3β2 for ACh (354 μM). They report similar, but less diverse, n_{app}'s for the two receptor subtypes (n_{app} = 1.4 for α3β2; n_{app} = 1.8 for α3β4). The reason for this discrepancy is unclear but most of the previous measurements, including data from a mammalian expression system (Wong et al., 1993), are consistent with our data.

The α3β2(229)·β4 chimera is anomalous because it displays a large, β4-like EC_{50} for ACh even though it includes regions of sequence that confer a β2-like EC_{50} in another chimera tested. Nonetheless, the α3β2(229)·β4 chimera exhibits a β2-like CYT/ACh response ratio and a β2-like irreversible block by neuronal bungarotoxin (Papke et al., 1993). Based on its agonist selectivity and affinity for neuronal bungarotoxin, we suggest that the large EC_{50} of this chimera arises from a change in the conformational states of the receptor that enhances the relative stability of the closed singly liganded receptor state (Koshland et al., 1966) rather than from a change in the agonist binding site.

Channel Block by the Agonist Fails to Account for Differences in the N_{app}

Measurements of the Hill coefficient at the foot of the dose-response relationship show that the differences between the n_{app}'s of the wild-type receptors are not due to channel block by the agonist because open-channel block is minimal in this region. However, open-channel block by the agonist could reduce the apparent EC_{50} of the agonist dose-response relationship. To assess the importance of this effect, we

calculated the dissociation constant K_i of agonist for an open-channel blocking site that would yield a β2-like EC_{50}, assuming that (*a*) the agonist can open all the channels (a worst-case analysis), (*b*) α3β2 and α3β4 display a β4-like EC_{50} for ACh (219 μM) in the absence of channel block, and (*c*) the n_{app} for α3β2 is ~1. The fractional response of the receptor (I_{peak}/I_{max}) under these conditions is

$$\frac{I_{peak}}{I_{max}} = \frac{1}{1 + \frac{219\ \mu M}{[ACh]} + \frac{[ACh]}{K_i}}.$$

A K_i of 10 μM would be required to bring the EC_{50} to 24 μM. Concentration- and voltage-jump experiments on neuronal nAChRs in bovine chromaffin cells suggest that the actual dissociation constant of ACh for the channel blocking site of neuronal nAChRs is closer to 700–1,400 μM (Maconochie and Knight, 1992), or 70- to 140-fold greater than the value required to bring the EC_{50} for α3β2 to 24 μM. Moreover, with a K_i of 10 μM, the maximum response would occur at ~50 μM ACh. Higher agonist concentrations would reduce the amplitude of the response, contrary to our data for α3β2 (Fig. 2*A*). Additionally, the sole substitution in M2, which is thought to contain the binding site for open-channel blockers, has no effect. These results strongly suggest that agonist self-block does not account for the differences in the EC_{50}'s that we observed.

Residues in a Homologous Region of γ and δ Determine Curare Binding

Three residue substitutions in the mouse γ and δ subunits (γ:Ile116↔δ:Val118, γ:Tyr117↔δ:Thr119, γ:Ser161↔δ:Lys163) account for a 10-fold increase in the affinity of the αβγ receptor over the αβδ receptor for the competitive antagonist (+)-dimethyltubocurarine (Sine, 1993). Residues β2:Ile118 and β2:Phe119 in the rat neuronal nicotinic receptor are homologous to γ:Ile116 and γ:Tyr117 in the mouse receptor and they are in the β2:104–120 domain of the rat neuronal nicotinic receptor. More recent evidence (Xie, Chiara, and Cohen, 1994) shows that the competitive antagonist *d*TC also photolabels residues γ:Tyr111 and γ:Tyr117 in the *Torpedo* nAChR (homologous to β2:Ser113 and β2:Phe119 in the rat neuronal nicotinic receptor). Thus, in a domain homologous to β2:104–120 in the rat neuronal nicotinic receptor, we find (*a*) residues in the *Torpedo* γ subunit that are photolabeled by *d*TC and (*b*) residues in the mouse γ and δ subunits that affect competitive antagonist binding. Residues in β2:104–120 affect the n_{app}, the EC_{50}, and agonist selectivity of neuronal nicotinic receptors. The proximity of residues in the muscle-type nicotinic receptors that affect binding and photolabeling by a competitive antagonist with those in the neuronal nicotinic receptor that affect the n_{app}, the EC_{50}, and agonist selectivity supports the hypothesis that residues β2:104–120 contribute to an α/β ligand binding site in neuronal nAChRs.

Differences in Channel Gating Do Not Account for Differences in the Wild-Type EC_{50}

We consider a simple sequential model to suggest that differences in agonist binding, rather than in the rates of conformational change, are primarily responsible for the

difference between the EC_{50}'s of α3β2 and α3β4 for ACh. This kinetic scheme (Scheme II) can be summarized as follows,

$$nA + R \overset{K_1^n}{\rightleftharpoons} C \overset{K_2}{\rightleftharpoons} O \overset{K_3}{\rightleftharpoons} I,$$

SCHEME II

where n is the Hill coefficient, A is the agonist, R is the free receptor, C is the closed agonist-bound receptor, O is the conducting state of the receptor, I is an agonist-bound inactivated state of the receptor, and K_1–K_3 are dissociation constants. At equilibrium, the fraction of open receptors P_o is,

$$P_o = \frac{1}{1 + \frac{1}{K_3} + K_2 + \frac{K_2 K_1^n}{[A]^n}}.$$

The EC_{50} is,

$$EC_{50} = K_1 \sqrt[n]{\frac{K_2 K_3}{1 + K_3 + K_3 K_2}}.$$

According to the data of Papke and Heinemann (1991), K_2 = 1.1 and 0.45, and K_3 = 10 and 20 for α3β2 and α3β4, respectively. The point here is not the absolute values of these numbers, but the fact that they differ by relatively small amounts for the two receptors. A similar conclusion is reached from our own kinetic data on voltage-jump relaxations, to be published separately. These differences would change the EC_{50} by less than twofold. Thus, differences in the cooperativity of binding and conformational transitions of α3β2 and α3β4 cannot account for the 20-fold difference we observed between the EC_{50}'s of the wild-type receptors for ACh. This model suggests that the wild-type dissociation constants for agonist binding (K_1's) differ by more than 10-fold.

Regardless of the particular kinetic model used, the differences between the mean open times of the α3β2 and α3β4 channels do not account for the differences in the EC_{50}'s of α3β2 and α3β4 for ACh. The open channel lifetime is usually interpreted as the rate constant for leaving the open state of the channel. The long open-channel lifetime of the primary α3β4 channel is 75% greater than the long open channel lifetime of the primary α3β2 channel (Papke et al., 1991). All else being equal, this difference in open channel lifetime would be associated with a smaller EC_{50} for α3β4 than for α3β2, contrary to the data.

Conclusions

Our study is the first attempt to determine the regions of sequence that account for the differences in the complete agonist dose-response relationship produced by two naturally occurring subunits of a channel. Past experiments on binding of antagonists or open-channel blockers have pinpointed just a few residues; however, channel activation in response to agonists is certainly a more complex phenomenon, involving binding, conformational changes, and interactions between the subunits. It

is therefore encouraging that clear trends emerge from the data. Our results emphasize the involvement of one region, β2:104–120, in the binding event and suggest that a broader region of sequence is involved in the subunit contacts and/or conformational changes that open the channel.

We thank Jeremy Gollub and Purnima Deshpande for technical assistance in oocyte injection and construction of some chimeras.

This work was supported by grants from the National Institute of Health (NS-11756) and from the California Tobacco-Related Disease Program (1RT-0365, 1RT-0286).

Original version received 25 May 1994 and accepted version received 10 February 1995.

REFERENCES

Blount, P., and J. P. Merlie. 1988. Native folding of an acetylcholine receptor α subunit expressed in the absence of other receptor subunits. *The Journal of Biological Chemistry.* 263:1072–1080.

Bormann, J. 1992. U-tube drug application. *In* Practical electrophysiological methods, a guide for in vitro studies in vertebrate neurobiology. H. Kettenmann and R. Grantyn, editors. Wiley-Liss, New York, NY. 136–140.

Cachelin, A. B., and R. Jaggi. 1991. β subunits determine the time course of desensitization in rat α3 neuronal nicotinic receptors. *Pflügers Archiv.* 419:579–582.

Chiara, D. C., and J. B. Cohen. 1992. Identification of amino acids contributing to high and low affinity *d*-tubocurarine sites on the *Torpedo* nicotinic acetylcholine receptor subunits. *FASEB Journal.* 6:A106. (Abstr.)

Cockcroft, V. B., D. J. Osguthorpe, E. A. Barnard, and G. G. Lunt. 1990. Modeling of agonist binding to the ligand-gated ion channel superfamily of receptors. *Proteins: Structure, Function, and Genetics.* 8:386–397.

Couturier, S., L. Erkman, S. Valera, D. Rungger, S. Bertrand, J. Boulter, M. Ballivet, and D. Bertrand. 1990. α5, α3, and non-α3: three clustered avian genes encoding neuronal nicotinic acetylcholine receptor-related subunits. *The Journal of Biological Chemistry.* 265:17560–17567.

Deneris, E. S., J. Connolly, S. W. Rogers, and R. Duvoisin. 1991. Pharmacological and functional diversity of neuronal nicotinic acetylcholine receptors. *Trends in Pharmacological Science.* 12:34–40.

Figl, A., B. N. Cohen, J. Gollub, N. Davidson, and H. A. Lester. 1993. Novel functional domains of the rat neuronal nicotinic β subunit. *Society for Neuroscience Abstracts.* 19:8. (Abstr.)

Figl, A., B. N. Cohen, M. W. Quick, N. Davidson, and H. A. Lester. 1992. Regions of β4·β2 subunit chimeras that contribute to the agonist selectivity of neuronal nicotinic receptors. *FEBS Letters.* 308:245–248.

Guastella, J. G., N. Nelson, H. Nelson, L. Czyzyk, S. Keynan, M. C. Midel, N. Davidson, H. A. Lester, and B. I. Kanner. 1990. Cloning and expression of a rat brain GABA transporter. *Science.* 249:1303–1306.

Higuchi, R. 1990. Recombinant PCR. *In* PCR protocols, a guide to methods and applications. M. A. Innis, D. H. Gelfand, J. J. Sninsky, and T. J. White, editors. Academic Press, Inc., San Diego, CA. 177–184.

Karlin, A. 1993. Structure of nicotinic acetylcholine receptors. *Current Opinion in Neurobiology.* 3:299–309.

Koshland, D. E., G. Neméthy, and D. Filmer. 1966. Comparison of experimental binding data and theoretical models in proteins containing subunits. *Biochemistry.* 5:365–385.

Leutje, C. W., and J. Patrick. 1991. Both α- and β-subunits contribute to the agonist sensitivity of neuronal nicotinic acetylcholine receptors. *The Journal of Neuroscience.* 11:837–845.

Leutje, C. W., M. Piattoni, and J. Patrick. 1993. Mapping of ligand binding sites of neuronal nicotinic acetylcholine receptors using chimeric α subunits. *Molecular Pharmacology.* 44:657–666.

Maconochie, D. J., and D. E. Knight. 1992. A study of the bovine adrenal chromaffin nicotinic receptor using patch clamp and concentration-jump techniques. *Journal of Physiology.* 454:129–153.

O'Leary, M. E., G. N. Filatov, and M. M. White. 1994. Characterization of the *d*-tubocurarine binding site of the *Torpedo* acetylcholine receptor. *The American Journal of Physiology.* In press.

Papke, R. L. 1993. The kinetic properties of neuronal nicotinic receptors: genetic basis of functional diversity. *Progress in Neurobiology.* 41:509–551.

Papke, R. L., R. M. Duvoisin, and S. F. Heinemann. 1993. The amino terminal half of the nicotinic β-subunit extracellular domain regulates the kinetics of inhibition by neuronal bungarotoxin. *Proceedings of the Royal Society of London B.* 252:141–148.

Papke, R. L., and S. F. Heinemann. 1991. The role of the β_4 subunit in determining the kinetic properties of rat neuronal nicotinic acetylcholine α_3-receptors. *Journal of Physiology.* 440:95–112.

Pedersen, S. E., and J. B. Cohen. 1990. d-Tubocurarine binding sites are located at the α-γ and α-δ subunit interfaces of the nicotinic acetylcholine receptor. *Proceedings of the National Academy of Sciences, USA.* 87:2785–2789.

Quick, M. W., and H. A. Lester. 1994. Methods for expression of excitability proteins in *Xenopus* oocytes. *In* Methods in Neurosciences. P. M. Conn, editor. Academic Press, San Diego, CA. 261–279.

Sine, S. M. 1993. Molecular dissection of subunit interfaces in the acetylcholine receptor: identification of residues that determine curare selectivity. *Proceedings of the National Academy of Sciences, USA.* 90:9436–9440.

Unwin, N. 1993. Neurotransmitter action: opening of ligand-gated ion channels *Neuron.* 10:31–41.

Vernino, S., M. Amador, C. W. Leutje, J. Patrick, and J. A. Dani. 1992. Calcium modulation and high calcium permeability of neuronal nicotinic acetylcholine receptors. *Neuron.* 8:127–134.

Wong, E. T., S. Mennerick, D. B. Clifford, C. F. Zorumski, and K. E. Isenberg. 1993. Expression of a recombinant neuronal nicotinic acetylcholine receptor in transfected HEK-293 cells. *Society for Neuroscience Abstracts.* 19:291. (Abstr.)

Xie, Y., D. C. Chiara, and J. B. Cohen. 1994. Mutational analysis of novel residues identified within the binding site of *d*-tubocurarine of *Torpedo* acetylcholine receptor. *International Symposium on Nicotine.* (Abstr.)